Published in final edited form as:
Cell. 2014 September 11; 158(6): 1335–1347. doi:10.1016/j.cell.2014.07.035.

Reelin Signaling Specifies the Molecular Identity of the Pyramidal Neuron Distal Dendritic Compartment

Justine V. Kupferman[1,2], **Jayeeta Basu**[2], **Marco J. Russo**[2], **Jenieve Guevarra**[1], **Stephanie K. Cheung**[2], and **Steven A. Siegelbaum**[2,3,4,*]

[1]Department of Biology, College of Physicians and Surgeons, Columbia University, 1051 Riverside Drive, New York, NY 10032, USA

[2]Department of Neuroscience, College of Physicians and Surgeons, Columbia University, 1051 Riverside Drive, New York, NY 10032, USA

[3]Department of Pharmacology Kavli Institute, College of Physicians and Surgeons, Columbia University, 1051 Riverside Drive, New York, NY 10032, USA

[4]Howard Hughes Medical Institute, College of Physicians and Surgeons, Columbia University, 1051 Riverside Drive, New York, NY 10032, USA

SUMMARY

The apical dendrites of many neurons contain proximal and distal compartments that receive synaptic inputs from different brain regions. These compartments also contain distinct complements of ion channels that enable the differential processing of their respective synaptic inputs, making them functionally distinct. At present, the molecular mechanisms that specify dendritic compartments are not well understood. Here, we report that the extracellular matrix protein Reelin, acting through its downstream, intracellular Dab1 and Src family tyrosine kinase signaling cascade, is essential for establishing and maintaining the molecular identity of the distal dendritic compartment of cortical pyramidal neurons. We find that Reelin signaling is required for the striking enrichment of HCN1 and GIRK1 channels in the distal tuft dendrites of both hippocampal CA1 and neocortical layer 5 pyramidal neurons, where the channels actively filter inputs targeted to these dendritic domains.

INTRODUCTION

Neuronal dendrites are elaborately branched structures that are divided into different compartments with distinct membrane properties and synaptic inputs (Lai and Jan, 2006; Larkum et al., 2009; Spruston, 2008). In CA1 pyramidal neurons (PNs) of the hippocampus, the proximal region of the apical dendrites, located in stratum radiatum (SR), receives excitatory input from CA3 PN axons through the Schaffer collateral (SC) pathway. In

*Correspondence: sas8@columbia.edu.

SUPPLEMENTAL INFORMATION

Supplemental Information includes Extended Experimental Procedures and seven figures and can be found with this article online at http://dx.doi.org/10.1016/j.cell.2014.07.035.

contrast, the CA1 PN distal dendritic tuft, located in stratum lacunosum moleculare (SLM), receives excitatory input from entorhinal cortex (EC) through the perforant path (PP). These two dendritic regions contain different sets of ion channels that allow these compartments to differentially process their synaptic inputs (Nicholson et al., 2006; Nusser, 2012).

One especially striking example of compartmental channel localization is provided by the distal dendritic enrichment of the HCN1 channels (Santoro et al., 1997; Lörincz et al., 2002; Notomi and Shigemoto, 2004), which contribute to the hyperpolarization-activated cation current, Ih, present in many neurons (Robinson and Siegelbaum, 2003). HCN1 is expressed in apical dendrites of PNs in subiculum, CA1, and neocortical layer 5 in a dramatic somatodendritic gradient where channel density increases as a function of distance from the soma, with the very distal dendritic tufts having as much as a 60-fold greater density compared with the soma (Lörincz et al., 2002).

In hippocampal CA1 PNs, the distal dendritic expression of HCN1 enables these channels to selectively regulate the synaptic response to the PP inputs from EC (Magee, 1999; Nolan et al., 2004). Deletion of HCN1 leads to an increase in amplitude and temporal summation of the PP excitatory postsynaptic potential (EPSP) and an enhancement in spatial learning and memory (Nolan et al., 2004). In contrast, HCN1 deletion has relatively little effect on dendritic integration of the SC EPSP, which is generated at more proximal regions of the CA1 PN dendrite where HCN1 expression is lower. These results suggest that HCN1 acts as a selective inhibitory constraint of hippocampal distal dendritic integration and of learning and memory.

While much progress has been made in elucidating the basic mechanisms of axon—dendrite polarity, little is known about the mechanisms that specify the distinct identities of dendritic compartments (Arnold, 2007; Kim et al., 2007). In the case of AMPA-type glutamate receptors, an increasing gradient of receptor expression as a function of distance along the apical dendrites of CA1 PNs in SR is thought to be cell-autonomous (Harnett et al., 2013; Shipman et al., 2013). However, the gradient of AMPA receptor density does not extend into the distal tuft dendrites in SLM (Nicholson et al., 2006). Images from previous studies indicate that the HCN1 dendritic gradient is not present in dissociated hippocampal neuron cultures (Noam et al., 2010). We thus explored the possibility that the localization of HCN1 to the distal tuft dendrites may be mediated by a non-cell-autonomous factor, focusing on the extracellular matrix glycoprotein Reelin, which is highly enriched in SLM (Alcántara et al., 1998, Ramos-Moreno et al., 2006).

Reelin is important for both neuronal migration and formation of cortical lamina in the developing brain (D'Arcangelo and Curran, 1998) and the innervation of CA1 dendrites in SLM by EC axons (Borrell et al., 2007). A spontaneous loss-of-function mutation in the ***reelin*** gene (the ***reeler*** mouse) leads to a number of brain abnormalities that result in uncoordinated movement (D'Arcangelo et al., 1995). Binding of Reelin to its two low-density lipoprotein receptors, the APOE receptor 2 and the VLDL receptor, activates Src family tyrosine kinases (SFKs) and the cytoplasmic signaling molecule Dab1. Dab1 activation in turn increases SFK activity, creating a positive feedback loop (Arnaud et al., 2003 Bock and Herz, 2003). Most of the actions of Reelin are thought to require signaling

through Dab1, whose deletion results in a ***reeler*** phenotype (Bock and Herz, 2003; D'Arcangelo et al.,1999; Sheldon et al., 1997). Like Reelin, Dab1 is localized to the CA1 SLM region in hippocampus (Borrell et al., 2007).

Reelin and Dab1 are also important for postnatal brain function as the expression of these proteins persists into adulthood (Alcántara et al., 1998). Disruption of Reelin signaling in the adult leads to altered synaptic signaling and plasticity (Trotter et al., 2013) and may contribute to neurological disease (Folsom and Fatemi, 2013). Here, we identify Reelin signaling via Dab1 and SFKs as a critical postnatal factor required for the enrichment of HCN1 in the distal tuft dendrites of both hippocampal CA1 and neocortical layer 5 PNs. As we find that Reelin signaling is also critical for the distal dendritic enrichment of GIRK1 channels, but is not required for expression of dendritic proteins not enriched in the distal dendrites, we suggest that the Reelin pathway plays a general role in establishing the molecular identity of the distal dendritic compartment.

RESULTS

HCN1 Distal Dendritic Enrichment Requires an Extrinsic Factor

To determine if the enrichment of HCN1 channels in CA1 PN distal dendrites depends on a cell autonomous mechanism, we examined HCN1 channel distribution in dissociated hippocampal neuronal cultures. Cultured neurons are capable of developing fundamental neuronal polarization by forming axons and both apical- and basal-like dendrites whose protein expression patterns mirror, in many instances, the in vivo patterns (Horton et al., 2006). Consistent with previous studies, HCN1 was expressed in the soma and dendrites of the dissociated neurons (Noam et al., 2010). However, there was no increase in HCN1 signal as a function of dendritic distance from the soma, suggesting that a non-cell-autonomous factor is involved in the distal enrichment of HCN1 (Figures S1A–S1D).

As a previous study reported that the EC inputs are required for distal HCN1 enrichment, we reexamined this mechanism by comparing HCN1 expression in organotypic hippocampal slice cultures either with or without cocultures of EC (Shin and Chetkovich, 2007). Organotypic cultures preserve much of the in vivo connectivity of the hippocampus (De Simoni et al., 2003) and are permissive for the distal dendritic enrichment of HCN1 (Shin and Chetkovich, 2007). However, in contrast to the results of Shin and Chetkovich (2007), we found that HCN1 was similarly enriched in the distal dendrites of CA1 PNs in the absence or presence of EC (Figures S1E–S1H; see Discussion for an explanation of the discrepancy).

One interesting possible non-cell-autonomous mechanism for HCN1 dendritic localization involves netrin G ligand-1 (NGL-1). A transsynaptic signaling molecule, NGL-1 is strongly expressed in CA1 PN distal dendrites and interacts with the netrin G1 receptor localized to EC axons. However, we found that mice with a deletion of NGL-1 (Nakashiba et al., 2002) showed a normal enrichment of HCN1 in the SLM region of CA1 (Figure S2).

Loss of Reelin or Dab1 Drastically Reduces HCN1 Localization in the Distal Dendrites

As both Reelin and its downstream partner Dab1 are enriched in SLM, we next explored the role of Reelin signaling in the distal dendritic enrichment of HCN1 by examining the brains of ***reeler*** mice. Genetic loss of Reelin caused a dramatic reduction in HCN1 staining in the CA1 ***SLM*** region (Figure S3). However, because the ***reeler*** mice display a number of developmental defects, including altered hippocampal structure, the loss of distal HCN1 may be a secondary result of abnormal dendritic morphology. We therefore adopted a strategy allowing for the cell-autonomous disruption of Reelin signaling in the postnatal hippocampus using a mouse line homozygous at a floxed allele of the ***Dab1*** gene (***Dab1$^{f/f}$*** mice) (Franco et al., 2011).

Dab1 expression was downregulated through unilateral injections in the hippocampus of newborn (P0/1) ***Dab1$^{f/f}$*** mice of a recombinant adeno-associated virus (rAAV) that expresses Cre-GFP. Four weeks after viral injection, strong Cre-GFP expression was observed in the soma of hippocampal neurons in the injected hemisphere, with few Cre-GFP + cells present in the hippocampus contralateral to the site of injection (Figure 1A).

In control (contralateral) hippocampal sections, Dab1 was highly enriched in SLM, in agreement with previous reports (Borrell et al., 2007) (Figure S4). In contrast, Dab1 levels were significantly reduced throughout CA1 in the hippocampus expressing Cre-GFP, with Dab1 intensity in SLM showing a strong negative correlation with somatic GFP intensity ($R^2 = 0.527$). There was no change in Dab1 levels in contralateral hippocampi (Figure S4). Importantly, hippocampal morphology, including CA1 PN dendritic structure (Figure S6), and synaptic transmission from CA3 to CA1 PNs (Figures 4 and S7) were unchanged following Dab1 knockdown, as long as Cre-GFP was not strongly overexpressed. As very high levels of Cre-GFP expression did lead to changes in hippocampal structure, including a widened CA1 PN cell body layer, we only analyzed results from brains with moderate levels of Cre-GFP showing normal hippocampal morphology.

We observed a dramatic reduction in HCN1 expression in the SLM region of CA1 in the hippocampus injected with AAV-Cre-GFP (Figures 1B–1F). In contrast, we found a normal pattern of HCN1 staining in the hippocampus contralateral to the site of viral injection. Moreover, the reduction in HCN1 was limited to SLM, with little change in the CA1 somatic layer or SR region. This suggests that Dab1 knockdown did not cause a general loss of channel protein. Similarly to Dab1 staining, HCN1 levels in SLM were strongly negatively correlated with somatic GFP intensity (Figure 1F). This correlation was observed both when comparing different hippocampi and when comparing different regions within a single hippocampus that differed in Cre-GFP expression, indicating that the effect of viral Dab1 knockdown was primarily cell autonomous. Dab1 knockdown also caused a reduction in distal enrichment of the HCN channel accessory subunit TRIP8b (Figure S5), which is important in the targeting of HCN1 to distal CA1 dendrites (Piskorowski et al., 2011; Lewis et al., 2009). Thus, disruption of Reelin signaling by viral knockdown of Dab1 or a loss-of-function Reelin mutation leads to a drastic impairment in the distal enrichment of HCN1 in the CA1 SLM region.

Dab1 Knockdown Selectively Affects Distally Enriched Proteins

To determine whether Reelin signaling is generally required for the enrichment of proteins in CA1 distal tuft dendrites, we examined the effect of Dab1 knockdown on the localization of the GIRK1 potassium channel subunit, which is also normally enriched in CA1 PN distal dendrites (Chen and Johnston, 2005; Drake et al., 1997). Dab1 knockdown caused a marked loss of GIRK1 staining from CA1 SLM, similar to our results with HCN1 (Figures 2A–2C). Furthermore, there was a strong negative correlation between GFP staining and GIRK1 levels ($R^2 = 0.682$).

Next, we explored whether Reelin signaling is required for targeting all proteins to distal dendrites or is specifically involved in targeting only those proteins that are enriched in distal dendrites. In contrast to our results with HCN1 and GIRK1, knockdown of Dab1 had no effect on the expression of two proteins normally present in a uniform distribution throughout the apical dendritic arbor. Thus there was no change in proximal or distal dendritic expression of either the cytoplasmic microtubule-associated protein MAP2 (Figures 2D–2F) or the GluR1 AMPA receptor subunit (Figures 2G–2I). In both cases there was only a weak correlation between somatic GFP intensity and MAP2 intensity in ***SLM*** ($R^2 = 0.237$) or GluR1 intensity (R2 = 0.323).

Our finding that MAP2 and GluR1 expression were unchanged argues that the loss of HCN1 and GIRK1 from distal dendrites is specific and is not a result of a general mistargeting of proteins to distal dendrites or disruption in dendritic structure. To determine directly whether dendritic morphology was altered by Dab1 knockdown, we examined reconstructions of Cre-GFP+ and Cre-GFP+ neurons in ***Dab1$^{f/f}$*** mice (Figure S6). We found no significant differences in dendritic morphology between control neurons (Cre-GFP−) and neurons in which Dab1 expression was reduced (Cre-GFP+), as measured by dendritic branching, total apical dendrite length, volume, or surface area. Thus, we conclude that postnatal Reelin/Dab1 signaling is required for the enrichment of specific classes of channels in the distal dendrites.

Ih Is Selectively Decreased in Distal Dendrites after Dab1 Knockdown

The light-microscopic immunohistochemistry results do not have the resolution to reveal whether there is a loss of HCN1 or GIRK1 channels in the cell membrane of the CA1 distal dendrites or whether HCN1 is depleted from an intracellular pool of channels. We therefore performed whole cell patch clamp recordings to provide a functional assay of levels of HCN channels and Ih in somatic, proximal dendritic (<150 μm from the soma), and distal dendritic (>250 μm from the soma) cell membranes in ***Dab1$^{f/f}$*** mice. Both Cre-GFP+ and Cre-GFP− neurons had similar action potential (AP) firing thresholds and peak AP amplitudes in both the soma and distal dendrites, indicating that the CA1 PNs and their dendrites were generally healthy in both control and Dab1 knockdown groups (Figures S7D–S7E).

We next used current clamp recordings to measure a number of CA1 PN electrophysiological properties previously shown to depend on levels of Ih, including resting membrane potential (RMP), input resistance (Rin) and voltage sag (Magee, 1998; Nolan et

al., 2004). Although, Dab1 knockdown caused no change in RMP or Rin in proximal dendrites, we observed a significant hyperpolarization of the RMP and a marked increase in Rin in the distal dendrites, consistent with a loss of Ih (Figures 3E and 3F).

To provide a more direct measure of Ih and HCN1 function, we next measured voltage sag, a depolarizing membrane response to hyperpolarizing current steps that is characteristic of the activation of Ih (Figure 3A). In recordings from proximal dendrites, voltage sag was not significantly altered following Dab1 knockdown (Figures 3A, 3B, and 3G). However, voltage sag was largely eliminated in the distal dendrites of Cre-GFP+ cells (Figures 3C and 3G). We confirmed that the voltage sag resulted from activation of Ih using the HCN channel blocker ZD7288, which caused a near complete block of voltage sag in Cre-GFP− distal dendrites, but had little effect on Cre-GFP+ PNs (Figures 3D and 3H–3J). These findings indicate a selective and near complete loss of Ih and membrane expression of HCN1 in CA1 PN distal dendrites following Dab1 knockdown.

The loss of voltage sag could result either from a loss of channel expression in the surface membrane or a negative shift in the voltage-dependence of Ih that opposes its activation during membrane hyperpolarization, as is observed following binding of the accessory subunit TRIP8b to the HCN channels (Santoro et al., 2009) or hydrolysis of PIP2 (Pian et al., 2006). However, we failed to observe any sag following Dab1 knockdown even when the membrane was hyperpolarized to voltages as negative as −160 mV, more than 80 mV negative to the voltage normally required to activate Ih, and far negative to the voltage shifts in Ih activation reported previously. Thus, we conclude that the loss of Ih likely reflects the loss of channel expression in the cell membrane.

Surprisingly, voltage sag at the soma was significantly increased by Dab1 knockdown, which also depolarized the somatic RMP (Figures 3E and 3G), indicative of an increase in somatic Ih. These results suggest that Reelin-Dab1 signaling is not generally required for membrane expression of HCN1 but rather is selectively involved in targeting HCN1 to the distal CA1 dendrites. The increase in somatic Ih following Dab1 knockdown may result from an increased pool of somatic HCN1 as a result of the channels being no longer targeted to the distal dendrites.

To investigate whether Dab1 knockdown also affected GIRK1 channel expression in the distal dendrite cell membrane, we measured the input resistance of distal dendrites from Cre-GFP+ and Cre-GFP− neurons before and after application of Ba^{2+}, a GIRK channel blocker (Harnett et al., 2013). In the absence of Ba^{2+}, the input resistance in the distal dendrites of Cre-GFP+ neurons was significantly higher than that of Cre-GFP− neurons, as observed above (Figure S7). In control Cre-GFP− neurons, Ba^{2+} significantly increased input resistance, as expected given the high levels of GIRK1 channels. Importantly, Ba^{2+} application failed to alter the input resistance of the Cre-GFP+ neurons, consistent with a loss of GIRK1 surface membrane expression in the distal dendrites. A loss of GIRK channels is also consistent with our findings that Dab1 knockdown increases Rin and shifts RMP to more negative values even when Ih is blocked with ZD7288 (Figures 3I and 3J).

As a further means of assaying changes in dendritic Ih, we examined the dendritic integration of the EPSPs evoked by electrical stimulation of PP and SC inputs to CA1 PNs. Previous studies have shown that the high density of Ih in the distal dendrites acts as an inhibitory shunt conductance that decreases the peak amplitude of PP EPSPs, speeds the time course of PP EPSP decay, and decreases the extent of PP EPSP temporal summation (Magee, 1998, 1999; Nolan et al., 2004). In contrast, Ih exerts a smaller effect on dendritic integration of SC inputs owing to the lower density of HCN1 channels in the proximal dendrites.

Whole cell recordings from the distal dendrites of CA1 PNs showed that the SC-evoked EPSPs were similar in magnitude in Cre-GFP+ and Cre-GFP− neurons (Figures 4B and 4C). However, Dab1 knockdown caused nearly a 2-fold increase in the PP EPSP peak amplitude (Figures 4D and 4E). Blockade of Ih with ZD7288 increased the EPSP evoked by PP stimulation in Cre-GFP+neurons, but did not alter EPSP size in Cre-GFP+ neurons. In addition, there was a marked increase in temporal summation during a brief burst of PP synaptic stimuli in Cre-GFP+ neurons compared to Cre-GFP− neurons. Furthermore, we found that ZD7288 significantly increased temporal summation in Cre-GFP− neurons but had no effect in Cre-GFP+ neurons (Figures 4F and 4G).

In total, our electrophysiological results reveal that Dab1 knockdown leads to a selective loss of HCN1 and GIRK1 channels from the cell membrane of distal dendrites in CA1 PNs, with little loss of HCN1 in proximal dendrites and an actual increase in the soma. Thus, we conclude that Dab1 signaling is not required for HCN1 and GIRK1 trafficking to the surface membrane but rather is important for the distal dendritic enrichment of these channels.

Reelin Is a Key Regulator of SFKs in the Postnatal Hippocampus

Are the effects of Reelin-Dab1 signaling on HCN1 expression mediated through Src family tyrosine kinases (SFKs), as described for other Reelin-Dab1 actions (Bock and Herz, 2003)? We examined the importance of SFK activation in HCN1 targeting using two antibodies, one that specifically recognizes the kinase active conformation of SFKs and one that recognizes both kinase active and inactive conformations (total SFK) (Gonfloni et al., 2000).

In both contralateral and Dab1 knockdown hippocampi, total SFK signal was high in SR and relatively low in SLM (Figures 5A–5C). In contrast, active SFK was highly enriched in SLM of CA1. Although Dab1 knockdown did not alter total SFK levels in any region of the dendrite, it markedly decreased active SFK levels in SLM (Figures 5D–5F). Western blots of hippocampal tissue with varying levels of Cre-GFP expression revealed a correlation between increased levels of GFP and reduced levels of active SFKs, with no changes in total SFK levels (Figure S4).

SFK Activity Is Required for HCN1 Surface Expression

The above results show that Reelin-Dab1 is important for activating SFKs. Next, we asked whether SFK activity is necessary for the proper dendritic targeting of HCN1. Because the SFK family members Src, Fyn, and Yes often functionally substitute for each other, and double mutant mice that lack Src and either Fyn or Yes die perinatally (Stein et al., 1994), we examined the role of SFK activity on the dendritic enrichment of HCN1 channels by

applying a pharmacological inhibitor of SFKs to organotypic hippocampal cultures. Such cultures are known to contain the essential components of the Reelin signaling pathway (Alvarez-Dolado et al., 1999; Del Río et al.,1996).

We first asked whether Reelin is necessary for the distal enrichment of HCN1 channels in organotypic cultures by adding receptor-associated protein (RAP) to the culture media. RAP is an intracellular chaperone for Reelin receptors that when applied extracellularly binds to the Reelin receptors, thereby preventing Reelin binding and activation of downstream signaling (Chen and Johnston, 2005; Gong et al., 2007). RAP treatment significantly reduced HCN1 staining intensity in the dendrites compared with GST controls (Figures 6A–6C) but did not significantly alter MAP2 staining (Figures 6A, 6B, and 6D), demonstrating that Reelin signaling is required for targeting of HCN1 to distal dendrites in organotypic cultures as well as in vivo.

We next investigated the role of SFKs in HCN1 distal enrichment by comparing the effects of the selective SFK inhibitor PP2 with its inert analog PP3. MAP2 staining intensity was not significantly different in cultures exposed to PP2 compared to cultures treated with PP3, indicating that SFK inhibition did not cause global changes in protein localization or dendritic structure (Figures 6E, 6F, and 6H). However, HCN1 staining was significantly reduced throughout CA1 in PP2-treated cultures, including in the cell body layer (Figures 6E–6G). This contrasts with our results using in vivo Dab1 knockdown or RAP treatment in organotypic cultures, where HCN1 intensity (and voltage sag) was reduced in distal dendrites but not in the somatic compartment. To address whether SFK inhibition results in a global loss of HCN1 surface expression, we performed somatic whole cell recordings from cultures treated with PP2 or PP3. Both PP2 and PP3-treated neurons fired action potentials similarly in response to depolarizing current injection (Figures 6I and 6J), indicating that the cultures were healthy. However, PP2 treatment, but not PP3 treatment, significantly reduced somatic voltage sag (Figure 6K). Thus, SFK activity appears to be required for both the distal enrichment of HCN1 and its surface membrane expression.

Dab1 Knockdown Reduces HCN1 in Distal Dendrites of Neocortical Layer 5 PNs

HCN1 is also highly enriched in the distal dendrites of neocortical layer 5 (L5) PNs, resulting in strong HCN1 staining in layer 1 (L1), the site of the PN distal tuft dendrites. Of interest, L1 also contains a population of Reelin-secreting interneurons, analogous to the Reelin-secreting neurons in SLM of CA1 (Ramos-Moreno and Clascá, 2013). To investigate if Reelin signaling is important for targeting HCN1 to distal dendrites in L5 PNs, we injected rAAV Cre-GFP into the neocortex of ***Dab1$^{f/f}$*** mice. Loss of Dab1 greatly reduced HCN1 staining in L1, compared with HCN1 expression in the control (contralateral) hemisphere (Figures 7A–7E). In contrast, MAP2 intensity was not altered by Cre-GFP expression (Figure 7F), again indicating that Reelin signaling is specifically required for the dendritic expression of proteins normally enriched in distal dendrites. Thus, we conclude that Reelin provides a general signal for specifying cortical PN distal dendritic identity, which is required for HCN1 localization.

Dab1 Knockdown in Adult Hippocampi Reduces HCN1 Levels in SLM

Is Reelin signaling selectively involved in the initial establishment of the proper pattern of HCN1 distal dendritic expression during early postnatal development or is it also important for the maintenance of HCN1 distal dendritic expression in the adult? To address this question, we injected rAAV Cre-GFP into the hippocampus of adult (~3 months of age) ***Dab1$^{f/f}$*** mice. We found that Dab1 knockdown in adult mice drastically reduced distal dendritic HCN1 in the hippocampal CA1 region (Figures 7G–7K), whereas MAP2 levels were unchanged (Figure 7L), demonstrating the importance of Reelin signaling throughout postnatal life.

DISCUSSION

Establishment of a Distal Dendritic Compartment

The distal tuft dendrites of both hippocampal CA1 and neocortical L5 PNs represent an electrophysiologically distinct compartment that actively filters the inputs to these locales. Here, we find that the extracellular matrix protein Reelin, acting through its downstream Dab1 and SFK signaling cascade, provides a non-cell-autonomous factor that specifies the identity of the distal dendritic compartment in both CA1 and L5 PNs. Thus, Reelin signaling is specifically required for the targeting of HCN1 and GIRK1 channels to the distal tuft dendrites, where they regulate the efficacy of dendritic integration.

Activity-Dependent and Independent Mechanisms of HCN1 Dendritic Targeting

A number of studies have examined HCN1 channel expression and trafficking are regulated. As no significant levels of HCN1 mRNA in dendrites have been so far reported (Santoro et al., 2000; Brewster et al., 2007; Cajigas et al., 2012), the channel is likely targeted to its cellular locale posttranslationally. Shin and Chetkovich (2007) concluded that the EC inputs to CA1 distal dendrites lead to HCN1 enrichment through an activity-dependent mechanism. This is consistent with findings that lesions of the EC input to CA1 result in HCN1 downregulation (Brauer et al., 2001). One possible mechanism by which EC inputs might regulate HCN1 expression and localization is through the synaptic excitation of calretinin-positive inhibitory neurons at the SR-SLM border in CA1, which may require activity for Reelin secretion (Chameau et al., 2009). Indeed, Reelin and Dab1 are present in organotypic cultures in both the presence and absence of EC (Alvarez-Dolado et al., 1999; Del Río et al., 1996). Although we failed to identify a requirement for EC inputs for HCN1 dendritic localization in organotypic cultures, it is possible that levels of interneuron activity under the conditions of our experiment may have triggered adequate levels of Reelin release without the need for EC input.

A second factor known to regulate HCN1 surface expression (Santoro et al., 2004, 2009) and dendritic targeting (Han et al., 2011; Piskorowski et al., 2011) is the brain-specific HCN channel auxiliary subunit TRIP8b. When the interaction between HCN1 and TRIP8b is prevented by deletion of the HCN1 conserved C-terminal tripeptide (Ser-Asn-Leu), the channels are no longer targeted to the distal dendrites and are uniformly expressed throughout the CA1 somatodendritic compartment (Piskorowski et al., 2011). However, TRIP8b alone is not sufficient for the distal enrichment of HCN1 channels as endogenous or

exogenous expression of TRIP8b in dissociated hippocampal neuron cultures fails to target HCN1 to the PN distal dendrites (Piskorowski et al., 2011).

Reelin Signaling in the Postnatal Hippocampus

Although Reelin signaling has been most thoroughly characterized during embryonic neuronal development, there is increasing evidence for a contribution of Reelin to synaptic function and cognition in the postnatal and adult hippocampus (Weeber et al., 2002, Beffert et al., 2005). For example, forebrain-specific deletion of Dab1 in adolescent mice (>1 month old) was shown to impair hippocampal synaptic function and spatial learning (Trotter et al., 2013).

Our results describe two roles for Reelin in the postnatal brain. First, we find that Reelin signaling plays a critical role in localizing both GIRK1 and HCN1 channels to the distal dendrites of PNs in both hippocampus and neocortex. Second, we show that Reelin is a major regulator of SFK activity in CA1 PN distal dendrites in SLM. This result is unexpected as SFKs can be activated by a wide variety of receptor pathways, including growth factor receptors, GPCRs, cadherins, and integrins and emphasizes the importance of Reelin for tyrosine kinase signaling in distal PN dendrites in the postnatal hippocampus (Parsons and Parsons, 2004).

The present results provide the first demonstration, to our knowledge, that Reelin signaling in the postnatal brain is critical for the dendritic localization and surface expression of nonsynaptic, voltage-gated ion channels. Moreover, our findings indicate that Reelin signaling plays a specific role in the dendritic localization of only those proteins that are normally enriched in the distal dendritic compartment. Thus, Reelin signaling is not required for dendritic targeting of proteins normally found in a generally uniform distribution throughout the apical dendrites. Based on these results, we conclude that Reelin signaling is important for specifying the identity of the distal dendritic compartment, both for hippocampal CA1 PNs and layer 5 neocortical neurons.

SFK Regulation of Ion Channel Surface Expression

How does the Reelin-Dab1 signaling cascade lead to the distal enrichment of HCN1? Our results suggest that local activation of SFKs likely plays a critical role, although it is unclear whether this represents a direct effect of tyrosine phosphorylation of HCN1 (and GIRK1) or occurs through some intermediary tyro-sine phosphoprotein. Previous studies have found that HCN channels may be directly regulated by SFKs, beginning with the initial cloning of the HCN channel gene family using a yeast two-hybrid screen for protein interactions with a domain of Src, the eponymous SFK (Santoro et al., 1997). Subsequent studies have shown that SFKs regulate both the gating and surface expression of HCN2 and HCN4 channels through phosphorylation of multiple tyrosine residues, many of which are conserved in HCN1 (Huang et al., 2008; Li et al., 2008; Lin et al., 2009; Zong et al., 2005). However, it is not yet known if HCN1 is directly phosphorylated by SFKs, or whether direct HCN1 channel tyrosine phosphorylation is required for its proper dendritic targeting.

In contrast to the specific role of Reelin and Dab1 signaling in the distal dendritic enrichment of HCN1, we find that SFK activity is important for the surface expression of

HCN1 throughout the somatodendritic domain of CA1 PNs. Chronic inhibition of SFK activity in organotypic cultures led to a near complete loss of HCN1 as measured both by immunohistochemistry and somatic voltage recordings. To account for the similarities and differences in the effects of SFK inhibition versus blockade of Reelin signaling, we hypothesize that SFK activity is required for proper surface expression of HCN1 throughout the somatodendritic compartment. Normally, the high concentration of Reelin in the SLM region of CA1 will lead to the strong localized activation of Dab1 and SFK in the distal dendrites of CA1 neurons, resulting in the distal dendritic enrichment of HCN1 and other proteins, including GIRK1. Factors distinct from Reelin may generate low levels of diffuse SFK activity in the soma and proximal dendrites that gives rise to the low but significant levels of HCN1 and Ih in these compartments. Thus, specific blockade of Reelin signaling blocks the enrichment of HCN1 and GIRK1 in the distal dendritic compartment, with little effect on protein levels in the soma and proximal dendrites. In contrast, indiscriminate blockade of SFK activity with the pharmacological inhibitor PP2 blocks tyrosine phosphorylation throughout the neuron, leading to a global loss of HCN1 and Ih. It will be of interest in the future to determine whether alterations in Reelin release and the somatodendritic pattern of SFK activity contribute to the redistribution of HCN1 following seizures (Jung et al., 2010; Powell et al., 2008). Future studies will also be important to address the molecular mechanisms by which Reelin, acting through SFKs, leads to enriched levels of HCN1 in the tuft dendrites.

EXPERIMENTAL PROCEDURES

Antibodies and Viruses

Please see the Extended Experimental Procedures for a list of antibodies, viruses, and animals used in this study.

Animals

All mouse lines were maintained in standard conditions in accordance with guidelines established by the NIH and by the Institutional Animal Care and Use Committee. C57B/6 wild-type mice were obtained from the Jackson Laboratory. ***Reeler*** knockout mice and wild-type littermates were purchased from the Jackson Laboratory (stock number 000235). $Dab1^{f/f}$ mice were generously provided by Gabriella D'Arcangelo at Rutgers University and Ulrich Mueller at the Scripps Research Institute. NGL1 knockout mice were a gift from Shigeyoshi Itohara at the Riken Institute.

Neonate Viral Injections

Perinatal rat pups were immersed in an ice-water bath for 8 to 10 min to achieve anesthesia. Pups were then gently wrapped in a Kimwipe and taped to the platform of a stereotactic injection apparatus. A glass pipette back-filled with rAAV was then lowered through the skull into the brain. Injection coordinates were 0.2 to 0.3 mm rostral to bregma and 0.2 to 0.4 mm lateral to the midline. Multiple injection depths were selected ranging from 0.2 to 0.05 mm below the cortical surface to ensure high infectivity throughout the hippocampus and cortex.

Electrophysiology

Standard current-clamp patch recordings were used to measure somatic and dendritic membrane properties and synaptic potentials. To minimize any voltage errors during large hyperpolarizing current steps during somatic and dendritic voltage recordings, the series resistance was compensated with the amplifier bridge circuit. As a result there was at most a 5 mV voltage error during the largest hyperpolarizing current steps (see Figure S7C). See Extended Experimental Procedures for detailed electrophysiology methods.

Organotypic Culture Preparation

Organotypic cultures were prepared from neonatal Sprague-Dawley rats (Charles River) at postnatal days 5–7 as previously described (Gogolla et al., 2006). In brief, rat pups were decapitated, and the brain was rapidly removed and placed in ice-cold Hank's balanced salt solution (HBSS) for 4 min. The hippocampi were dissected out and chopped along the transverse axis into 400 μM sections with a McIlwain tissue chopper (Stoelting). Sections were gently transferred with a paintbrush to organotypic culture inserts (Millipore) in High Serum Media (50% DMEM with Glutamax, 25% heat-inactivated donor equine serum, 25% HBSS, 10 mM HEPES). Media was exchanged every 2 to 3 days with fresh High Serum Media.

All experimental treatments in organotypic cultures began on day in vitro (DIV) 8 and were terminated after 48 hr on DIV 10. The following drugs were used: PP2 (5 μM, Tocris), PP3 (5 μM, Tocris), GST-RAP (50 μg/ml, Enzo Scientific), and GST-GABARAP (50 μg/ml, Enzo Scientific).

Imaging and Analysis

Images were acquired on a Zeiss LSM700 scanning confocal microscope. Maximum intensity projections were created using ImageJ. To display larger brain regions in representative images, maximum intensity z projections were stitched together using the Zeiss software tiling feature. For all quantitative analyses, maximum intensity z projections of single (not tiled) fields of view taken using the 20X objective (0.8 na) were used. Imaging settings (pinhole size, laser power and gain, etc.) were identical for each experiment. Square ROIs were chosen to encompass the PN soma in SP, central SR (half the distance between SP and SLM), and SLM. ROI size was kept consistent for each experiment. For netrin-G ligand mice experiments, imaging and analysis was performed as described, but using a BioRad MRC confocal microscope.

Neurons were traced and Sholl analysis was performed using NeuroLucida Software (MicroBrightField).

Statistical analysis was done using Prism. Unless otherwise indicated p values are from unpaired t tests given with standard errors of the mean (SEM); all p values (significance level set at $p<0.05$) for t-tests are two tailed and all ANOVAs were corrected for multiple comparisons post-hoc tests as indicated. Figures were assembled with Adobe Illustrator.

Supplementary Material

Refer to Web version on PubMed Central for supplementary material.

Acknowledgments

We thank Rebecca Piskorowski, Vivien Chevaleyre, Fred Hitti, and Christine Denny for helpful discussions and invaluable advice. We thank Haiying Liu for expert technical assistance. We are indebted to Beth Crowell, Gabriella D'Arcangelo, Ulrich Müller, Shigeyoshi Itohara, Justin Trotter, and Ed Weeber for sharing information, animals and reagents. We also thank Bina Santoro and Arjun Masurkar for very helpful comments on the manuscript. Funding was provided by NIH grants T32 GM008798 and R01 NS036658 and from the Howard Hughes Medical Institute.

References

Alcántara S, Ruiz M, D'Arcangelo G, Ezan F, de Lecea L, Curran T, Sotelo C, Soriano E. Regional and cellular patterns of reelin mRNA expression in the forebrain of the developing and adult mouse. J Neurosci. 1998; 18:7779–7799. [PubMed: 9742148]

Alvarez-Dolado M, Ruiz M, Del Río JA, Alcántara S, Burgaya F, Sheldon M, Nakajima K, Bernal J, Howell BW, Curran T, et al. Thyroid hormone regulates reelin and dab1 expression during brain development. J Neurosci. 1999; 19:6979–6993. [PubMed: 10436054]

Arnaud L, Ballif BA, Forster E, Cooper JA. Fyn tyrosine kinase is a critical regulator of disabled-1 during brain development. Curr Biol. 2003; 13:9–17. [PubMed: 12526739]

Arnold DB. Polarized targeting of ion channels in neurons. Pflugers Arch. 2007; 453:763–769. [PubMed: 17091311]

Beffert U, Weeber EJ, Durudas A, Qiu S, Masiulis I, Sweatt JD, Li WP, Adelmann G, Frotscher M, Hammer RE, Herz J. Modulation of synaptic plasticity and memory by Reelin involves differential splicing of the lipoprotein receptor Apoer2. Neuron. 2005; 47:567–579. [PubMed: 16102539]

Bock HH, Herz J. Reelin activates SRC family tyrosine kinases in neurons. Curr Biol. 2003; 13:18–26. [PubMed: 12526740]

Borrell V, Pujadas L, Simó S, Durà D, Solé M, Cooper JA, Del Río JA, Soriano E. Reelin and mDab1 regulate the development of hippocampal connections. Mol Cell Neurosci. 2007; 36:158–173. [PubMed: 17720534]

Brauer AU, Savaskan NE, Kole MH, Plaschke M, Monteggia LM, Nestler EJ, Simburger E, Deisz RA, Ninnemann O, Nitsch R. Molecular and functional analysis of hyperpolarization-activated pacemaker channels in the hippocampus after entorhinal cortex lesion. FASEB. 2001; 15:2689–2701.

Brewster AL, Chen Y, Bender RA, Yeh A, Shigemoto R, Baram TZ. Quantitative analysis and subcellular distribution of mRNA and protein expression of the hyperpolarization-activated cyclic nucleotide-gated channels throughout development in rat hippocampus. Cereb Cortex. 2007; 17:702–712. [PubMed: 16648453]

Cajigas IJ, Tushev G, Will TJ, tom Dieck S, Fuerst N, Schuman EM. The local transcriptome in the synaptic neuropil revealed by deep sequencing and high-resolution imaging. Neuron. 2012; 74:453–466. [PubMed: 22578497]

Chameau P, Inta D, Vitalis T, Monyer H, Wadman WJ, van Hooft JA. The N-terminal region of reelin regulates postnatal dendritic maturation of cortical pyramidal neurons. Proc Natl Acad Sci USA. 2009; 106:7227–7232. [PubMed: 19366679]

Chen X, Johnston D. Constitutively active G-protein-gated inwardly rectifying K+ channels in dendrites of hippocampal CA1 pyramidal neurons. J Neurosci. 2005; 25:3787–3792. [PubMed: 15829630]

D'Arcangelo G, Curran T. Reeler: new tales on an old mutant mouse. BioEssays. 1998; 20:235–244. [PubMed: 9631651]

D'Arcangelo G, Miao GG, Chen SC, Soares HD, Morgan JI, Curran T. A protein related to extracellular matrix proteins deleted in the mouse mutant reeler. Nature. 1995; 374:719–723. [PubMed: 7715726]

D'Arcangelo G, Homayouni R, Keshvara L, Rice DS, Sheldon M, Curran T. Reelin is a ligand for lipoprotein receptors. Neuron. 1999; 24:471–479. [PubMed: 10571240]

De Simoni A, Griesinger CB, Edwards FA. Development of rat CA1 neurones in acute versus organotypic slices: role of experience in synaptic morphology and activity. J Physiol. 2003; 550:135–147. [PubMed: 12879864]

Del Río JA, Heimrich B, Supèr H, Borrell V, Frotscher M, Soriano E. Differential survival of Cajal-Retzius cells in organotypic cultures of hippocampus and neocortex. J Neurosci. 1996; 16:6896–6907. [PubMed: 8824328]

Drake CT, Bausch SB, Milner TA, Chavkin C. GIRK1 immunoreactivity is present predominantly in dendrites, dendritic spines, and somata in the CA1 region of the hippocampus. Proc Natl Acad Sci USA. 1997; 94:1007–1012. [PubMed: 9023373]

Folsom TD, Fatemi SH. The involvement of Reelin in neurode-velopmental disorders. Neuropharmacology. 2013; 68:122–135. [PubMed: 22981949]

Franco SJ, Martinez-Garay I, Gil-Sanz C, Harkins-Perry SR, Müller U. Reelin regulates cadherin function via Dab1/Rap1 to control neuronal migration and lamination in the neocortex. Neuron. 2011; 69:482–497. [PubMed: 21315259]

Gogolla N, Galimberti I, DePaola V, Caroni P. Preparation of organotypic hippocampal slice cultures for long-term live imaging. Nature Prot. 2006; 1:1165–1171.

Gonfloni S, Weijland A, Kretzschmar J, Superti-Furga G. Crosstalk between the catalytic and regulatory domains allows bidirectional regulation of Src. Nat Struct Biol. 2000; 7:281–286. [PubMed: 10742171]

Gong C, Wang TW, Huang HS, Parent JM. Reelin regulates neuronal progenitor migration in intact and epileptic hippocampus. J Neurosci. 2007; 27:1803–1811. [PubMed: 17314278]

Han Y, Noam Y, Lewis AS, Gallagher JJ, Wadman WJ, Baram TZ, Chetkovich DM. Trafficking and gating of hyperpolarization-activated cyclic nucleotide-gated channels are regulated by interaction with tetra-tricopeptide repeat-containing Rab8b-interacting protein (TRIP8b) and cyclic AMP at distinct sites. J Biol Chem. 2011; 286:20823–20834. [PubMed: 21504900]

Harnett MT, Xu NL, Magee JC, Williams SR. Potassium channels control the interaction between active dendritic integration compartments in layer 5 cortical pyramidal neurons. Neuron. 2013; 79:516–529. [PubMed: 23931999]

Horton AC, Yi JJ, Ehlers MD. Cell type-specific dendritic polarity in the absence of spatially organized external cues. Brain Cell Biol. 2006; 35:29–38. [PubMed: 17940911]

Huang J, Huang A, Zhang Q, Lin YC, Yu HG. Novel mechanism for suppression of hyperpolarization-activated cyclic nucleotide-gated pacemaker channels by receptor-like tyrosine phosphatase-alpha. J Biol Chem. 2008; 283:29912–29919. [PubMed: 18768480]

Jung S, Bullis JB, Lau IH, Jones TD, Warner LN, Poolos NP. Downregulation of dendritic HCN channel gating in epilepsy is mediated by altered phosphorylation signaling. J Neurosci. 2010; 30:6678–6688. [PubMed: 20463230]

Kim J, Jung SC, Clemens AM, Petralia RS, Hoffman DA. Regulation of dendritic excitability by activity-dependent trafficking of the A-type K+ channel subunit Kv4.2 in hippocampal neurons. Neuron. 2007; 54:933–947. [PubMed: 17582333]

Lai HC, Jan LY. The distribution and targeting of neuronal voltage-gated ion channels. Nat Rev Neurosci. 2006; 7:548–562. [PubMed: 16791144]

Larkum ME, Nevian T, Sandler M, Polsky A, Schiller J. Synaptic integration in tuft dendrites of layer 5 pyramidal neurons: a new unifying principle. Science. 2009; 325:756–760. [PubMed: 19661433]

Lewis AS, Schwartz E, Chan CS, Noam Y, Shin M, Wadman WJ, Surmeier DJ, Baram TZ, Macdonald RL, Chetkovich DM. Alternatively spliced isoforms of TRIP8b differentially control h channel trafficking and function. J Neurosci. 2009; 29:6250–6265. [PubMed: 19439603]

Li CH, Zhang Q, Teng B, Mustafa SJ, Huang JY, Yu HG. Src tyrosine kinase alters gating of hyperpolarization-activated HCN4 pacemaker channel through Tyr531. Am J Physiol Cell Physiol. 2008; 294:C355–C362. [PubMed: 17977941]

Lin YC, Huang J, Kan H, Frisbee JC, Yu HG. Rescue of a trafficking defective human pacemaker channel via a novel mechanism: roles of Src, Fyn, and Yes tyrosine kinases. J Biol Chem. 2009; 284:30433–30440. [PubMed: 19748888]

Lörincz A, Notomi T, Tamás G, Shigemoto R, Nusser Z. Polarized and compartment-dependent distribution of HCN1 in pyramidal cell dendrites. Nat Neurosci. 2002; 5:1185–1193. [PubMed: 12389030]

Magee JC. Dendritic hyperpolarization-activated currents modify the integrative properties of hippocampal CA1 pyramidal neurons. J Neurosci. 1998; 18:7613–7624. [PubMed: 9742133]

Magee JC. Dendritic lh normalizes temporal summation in hippocampal CA1 neurons. Nat Neurosci. 1999; 2:508–514. [PubMed: 10448214]

Nakashiba T, Nishimura S, Ikeda T, Itohara S. Complementary expression and neurite outgrowth activity of netrin-G subfamily members. Mech Dev. 2002; 111:47–60. [PubMed: 11804778]

Nicholson DA, Trana R, Katz Y, Kath WL, Spruston N, Geinisman Y. Distance-dependent differences in synapse number and AMPA receptor expression in hippocampal CA1 pyramidal neurons. Neuron. 2006; 50:431–442. [PubMed: 16675397]

Noam Y, Zha Q, Phan L, Wu RL, Chetkovich DM, Wadman WJ, Baram TZ. Trafficking and surface expression of hyperpolarization-activated cyclic nucleotide-gated channels in hippocampal neurons. J Biol Chem. 2010; 285:14724–14736. [PubMed: 20215108]

Nolan MF, Malleret G, Dudman JT, Buhl DL, Santoro B, Gibbs E, Vronskaya S, Buzsáki G, Siegelbaum SA, Kandel ER, Morozov A. A behavioral role for dendritic integration: HCN1 channels constrain spatial memory and plasticity at inputs to distal dendrites of CA1 pyramidal neurons. Cell. 2004; 119:719–732. [PubMed: 15550252]

Notomi T, Shigemoto R. Immunohistochemical localization of Ih channel subunits, HCN1-4, in the rat brain. J Comp Neurol. 2004; 471:241–276. [PubMed: 14991560]

Nusser Z. Differential subcellular distribution of ion channels and the diversity of neuronal function. Curr Opin Neurobiol. 2012; 22:366–371. [PubMed: 22033281]

Parsons SJ, Parsons JT. Src family kinases, key regulators of signal transduction. Oncogene. 2004; 23:7906–7909. [PubMed: 15489908]

Pian P, Bucchi A, Robinson RB, Siegelbaum SA. Regulation of gating and rundown of HCN hyperpolarization-activated channels by exogenous and endogenous PIP2. J Gen Physiol. 2006; 128:593–604. [PubMed: 17074978]

Piskorowski R, Santoro B, Siegelbaum SA. TRIP8b splice forms act in concert to regulate the localization and expression of HCN1 channels in CA1 pyramidal neurons. Neuron. 2011; 70:495–509. [PubMed: 21555075]

Powell KL, Ng C, O'Brien TJ, Xu SH, Williams DA, Foote SJ, Reid CA. Decreases in HCN mRNA expression in the hippocampus after kindling and status epilepticus in adult rats. Epilepsia. 2008; 49:1686–1695. [PubMed: 18397293]

Ramos-Moreno, T.; Clascá, F. Quantitative mapping of the local and extrinsic sources of GABA and Reelin to the layer Ia neuropil in the adult rat neocortex. Brain Struct Funct. 2013. Published online July 2, 2013 http://dx.doi.org/10.1007/s00429-013-0591-x

Ramos-Moreno T, Galazo MJ, Porrero C, Martínez-Cerdeño V, Clascá F. Extracellular matrix molecules and synaptic plasticity: immunomapping of intracellular and secreted Reelin in the adult rat brain. Eur J Neurosci. 2006; 23:401–422. [PubMed: 16420448]

Robinson RB, Siegelbaum SA. Hyperpolarization-activated cation currents: from molecules to physiological function. Annu Rev Physiol. 2003; 65:453–480. [PubMed: 12471170]

Santoro B, Grant SG, Bartsch D, Kandel ER. Interactive cloning with the SH3 domain of N-src identifies a new brain specific ion channel protein, with homology to eag and cyclic nucleotide-gated channels. Proc Natl Acad Sci USA. 1997; 94:14815–14820. [PubMed: 9405696]

Santoro B, Chen S, Luthi A, Pavlidis P, Shumyatsky GP, Tibbs GR, Siegelbaum SA. Molecular and functional heterogeneity of hyperpolarization-activated pacemaker channels in the mouse CNS. J Neurosci. 2000; 20:5264–5275. [PubMed: 10884310]

Santoro B, Wainger BJ, Siegelbaum SA. Regulation of HCN channel surface expression by a novel C-terminal protein-protein interaction. J Neurosci. 2004; 24:10750–10762. [PubMed: 15564593]

Santoro B, Piskorowski RA, Pian P, Hu L, Liu H, Siegelbaum SA. TRIP8b splice variants form a family of auxiliary subunits that regulate gating and trafficking of HCN channels in the brain. Neuron. 2009; 62:802–813. [PubMed: 19555649]

Sheldon M, Rice DS, D'Arcangelo G, Yoneshima H, Nakajima K, Mikoshiba K, Howell BW, Cooper JA, Goldowitz D, Curran T. Scrambler and yotari disrupt the disabled gene and produce a reeler-like phenotype in mice. Nature. 1997; 389:730–733. [PubMed: 9338784]

Shin M, Chetkovich DM. Activity-dependent regulation of h channel distribution in hippocampal CA1 pyramidal neurons. J Biol Chem. 2007; 282:33168–33180. [PubMed: 17848552]

Shipman SL, Herring BE, Suh YH, Roche KW, Nicoll RA. Distance-dependent scaling of AMPARs is cell-autonomous and GluA2 dependent. J Neurosci. 2013; 33:13312–13319. [PubMed: 23946389]

Spruston N. Pyramidal neurons: dendritic structure and synaptic integration. Nat Rev Neurosci. 2008; 9:206–221. [PubMed: 18270515]

Stein PL, Vogel H, Soriano P. Combined deficiencies of Src, Fyn, and Yes tyrosine kinases in mutant mice. Genes Dev. 1994; 8:1999–2007. [PubMed: 7958873]

Trotter J, Lee GH, Kazdoba TM, Crowell B, Domogauer J, Mahoney HM, Franco SJ, Müller U, Weeber EJ, D'Arcangelo G. Dab1 is required for synaptic plasticity and associative learning. J Neurosci. 2013; 33:15652–15668. [PubMed: 24068831]

Weeber EJ, Beffert U, Jones C, Christian JM, Forster E, Sweatt JD, Herz J. Reelin and ApoE receptors cooperate to enhance hippocampal synaptic plasticity and learning. J Biol Chem. 2002; 277:39944–39952. [PubMed: 12167620]

Zong X, Eckert C, Yuan H, Wahl-Schott C, Abicht H, Fang L, Li R, Mistrik P, Gerstner A, Much B, et al. A novel mechanism of modulation of hyperpolarization-activated cyclic nucleotide-gated channels by Src kinase. J Biol Chem. 2005; 280:34224–34232. [PubMed: 16079136]

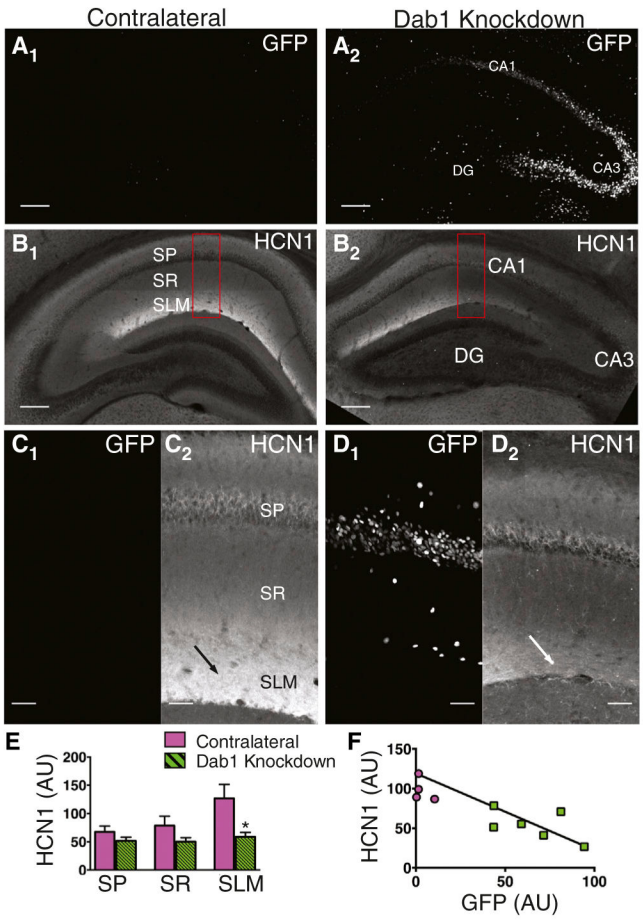

Figure 1. Knockdown of Dab1 Disrupts HCN1 Enrichment in Distal Dendrites of Hippocampal CA1 PNs

(A) Cre-GFP signal in a control hippocampus in the hemisphere contralateral to site of rAAV Cre-GFP injection (A_1) and a Dab1 knockdown hippocampus in the injected hemisphere. CA1, CA3, and dentate gyrus (DG) are labeled. To show the entire hippocampal structure in the figure low magnification (5X) images of maximum intensity z projections were tiled. See experimental procedures for imaging details. Scale bar, 200 μm.

(B) HCN1 intensity was greatest in the CA1 SLM in the contralateral control hippocampus (B_1). HCN1 staining intensity was reduced in the Dab1 knock-down hippocampus (B_2). Red rectangles indicate regions shown in (C). Scale bar, 200 μm.

(C) High-magnification image of GFP signal (C_1) and HCN1 staining (C_2) in CA1 region of contralateral hippocampus. To show details of CA1 region high magnification (20X) images of maximum intensity z projections were tiled. Arrow points to region of high HCN1 signal in SLM. Scale bar, 50 μm.

(D) High-magnification image of GFP signal (D_1) and HCN1 staining (D_2) in CA1 region of Dab1 knockdown hippocampus. Arrow points to region of reduced HCN1 signal in SLM. Scale bar, 50 μm.

(E) Mean HCN1 intensity in contralateral (magenta bars) and Dab1 knockdown (green striped bars) hippocampi. A significant decrease in HCN1 staining was only found in SLM (SP, $p = 0.101$; SR, $p = 0.194$; SLM $p = 0.010$). All p values ± SEM were generated from

unpaired t tests unless otherwise noted. (F) Plot of HCN1 intensity versus GFP intensity (R^2 = 0.552).

See also Figures S1, S2, S3, and S4.

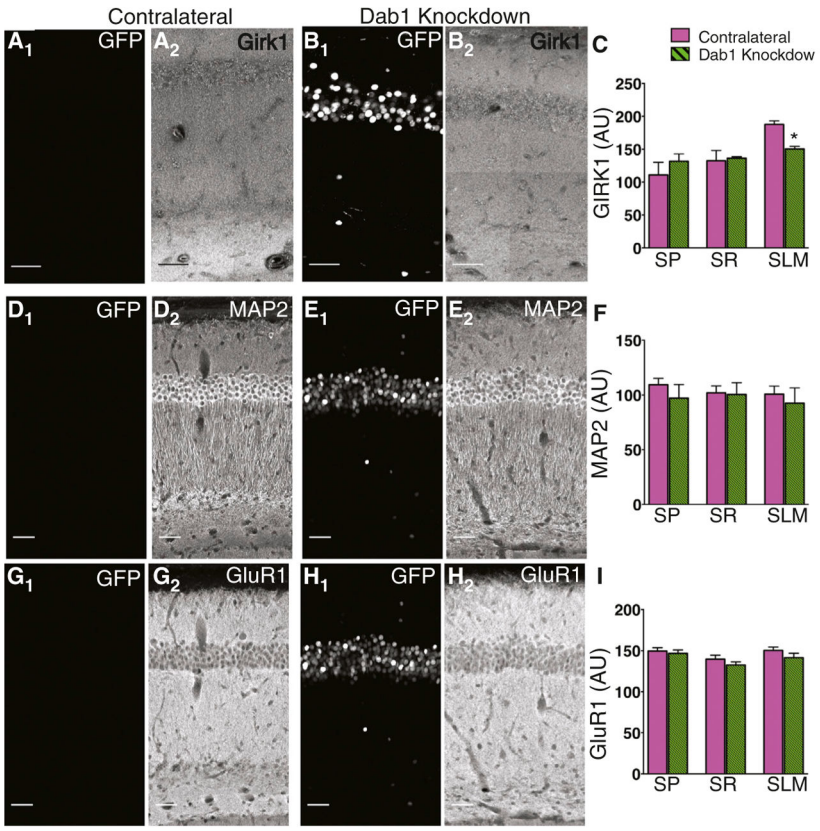

Figure 2. Knockdown of Dab1 Does Not Alter Localization of Proteins with a Uniform Dendritic Protein Distribution

(A) GFP signal (A_1) and GIRK1 staining (A_2) in the hippocampus contralateral to site of injection. To show details of CA1 maximum intensity z projections were tiled. Scale bar, 50 μm for all images.

(B) GFP signal (B_1) and GIRK1 staining (B_2) in Dab1 knockdown hippocampus ipsilateral to site of injection.

(C) Mean GIRK1 staining in contralateral and Dab1 knockdown hippocampi. Dab1 knockdown caused a significant reduction in GIRK1 staining intensity in ***SLM*** ($p = 0.001$).

(D) GFP signal (D_1) and MAP2 staining (D_2) in contralateral hippocampus.

(E) GFP signal (E_1) and MAP2 staining (E_2) in Dab1 knockdown hippocampi.

(F) Mean intensity of MAP2 staining was unaltered by Dab1 knockdown in all layers of CA1 ($p > 0.05$).

(G) GFP signal (G_1) and GluR1 staining (G_2) in contralateral hippocampus.

(H) GFP signal (H_1) and GluR1 staining (H_2) in Dab1 knockdown hippocampi.

(I) Mean intensity of GluR1 staining was unaltered by Dab1 knockdown ($p > 0.05$).

See also Figures S5 and S6.

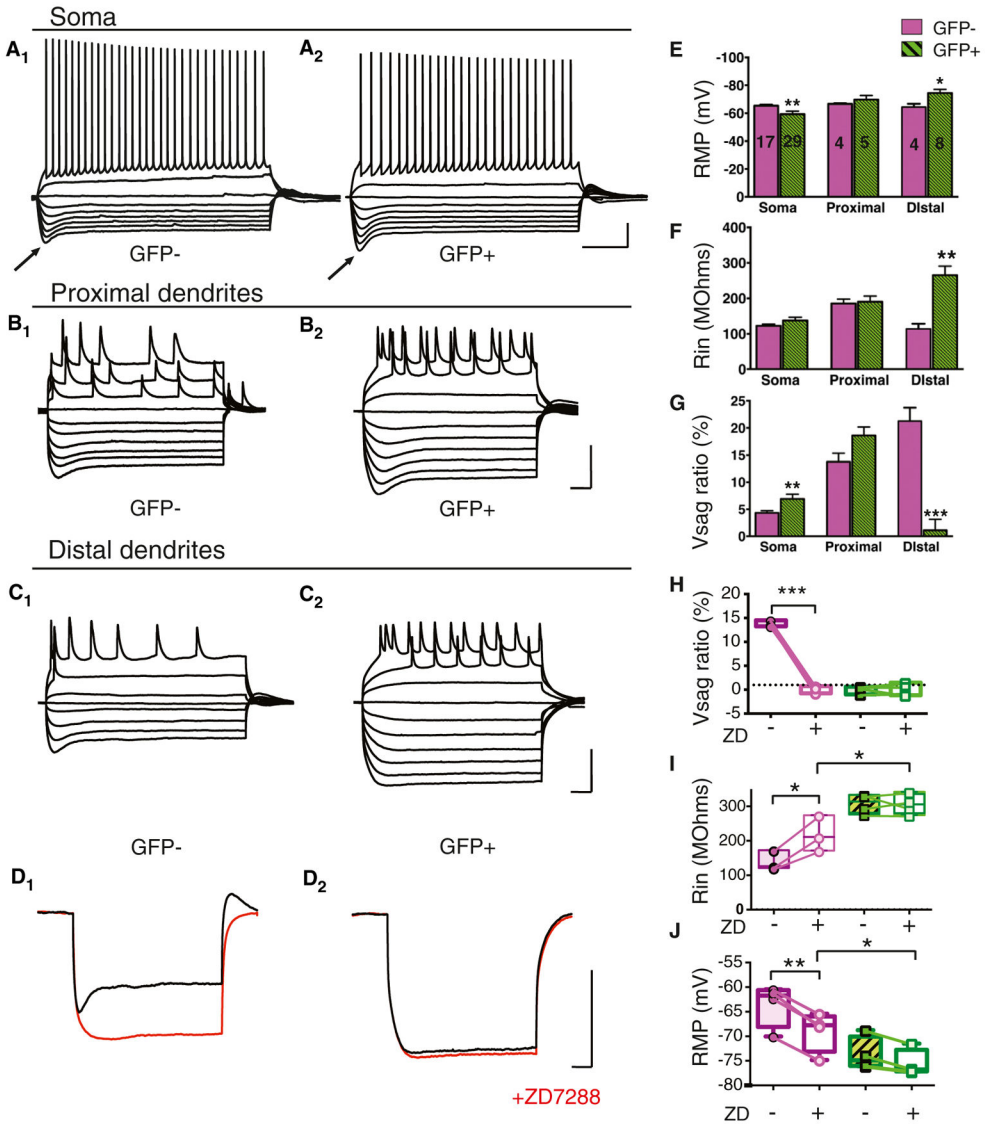

Figure 3. Dab1 Knockdown Reduces Ih Selectively in Distal Dendrites of CA1 PNs

(A) Whole cell current clamp voltage recordings from soma of Cre-GFP− (A_1) and Cre-GFP + (A_2) CA1 PNs. Voltage responses are shown to a series of hyperpolarizing and depolarizing current pulses. Arrows point to pronounced voltage sag following strongest hyperpolarization responses in Cre-GFP−and Cre-GFP+ neurons. Scale bars represent 20 mV, 0.2 s.

(B) Whole cell current clamp recordings from proximal dendrites of Cre-GFP− (B_1) and Cre-GFP+ (B_2) CA1 neurons. Scale bars, 50 mV, 0.1 s.

(C) Whole cell current clamp recordings from distal dendrites of Cre-GFP− (C_1) and Cre-GFP+ (C_2) CA1 neurons. Scale bars, 50 mV, 0.1 s. Note pronounced voltage sag with strongest hyperpolarizations in recordings from GFP- but not GFP+ PN distal dendrites.

(D) Whole cell current clamp voltage recordings from distal dendrites in Cre-GFP− (D_1) and Cre-GFP+ (D_2) neurons before (black traces) and after application of 10 μM ZD7288 (red traces). Scale bars, 50 mV, 0.1 s.

(E) Resting membrane potential (RMP in mV) of Cre-GFP− (control, magenta) and Cre-GFP+ (Dab1 knockdown, green) neurons. Dab1 knockdown caused a significant negative shift in the RMP in distal dendrites ($p = 0.036$) and a significant positive shift in RMP in the soma ($p = 0.006$). Number of cells for each condition are displayed on graph.

(F) Dab1 knockdown caused a significant increase in mean input resistance (Rin) selectively in distal dendrites ($p = 0.003$).

(G) Dab1 knockdown significantly increased the voltage sag ratio (V_{sag} ratio) in the soma ($p = 0.004$) and significantly decreased V_{sag} ratio in the distal dendrites ($p = 0.0002$). V_{sag} ratio was measured as $(V_{peak} - V_{steady\text{-}state})/V_{peak} \times 100\%$, where V_{peak} is the maximal hyperpolarized voltage and $V_{steady\text{-}state}$ is the steady-state voltage in response to a given hyperpolarizing current step relative to membrane holding potential.

(H) V_{sag} ratio measured in distal dendrites of Cre-GFP− and Cre-GFP+ neurons before and after application of ZD7288. ZD7288 significantly decreased sag only in Cre-GFP− neurons (paired t test, $p < 0.0001$). Plot shows individual cells, min to max (whiskers), median (line), and 25^{th} to 75^{th} percentiles (box).

(I) Rin measured in distal dendrites of Cre-GFP− and Cre-GFP+ neurons before and after application of ZD7288. ZD7288 significantly increased Rin in Cre-GFP− neurons (paired t test, $p < 0.0001$). In the presence of ZD7288, Rin was significantly greater in Cre-GFP+ neurons than in Cre-GFP− neurons ($p = 0.035$). (J) RMP in distal dendrites of Cre-GFP− and Cre-GFP+ neurons before and after application of ZD7288 (red traces). ZD7288 caused a significant negative shift in the RMP of Cre-GFP− neurons (paired t test, $p = 0.001$). In the presence of ZD7288, RMP was significantly more negative in Cre-GFP+ neurons than in GFP-neurons ($p = 0.036$).

See also Figure S7.

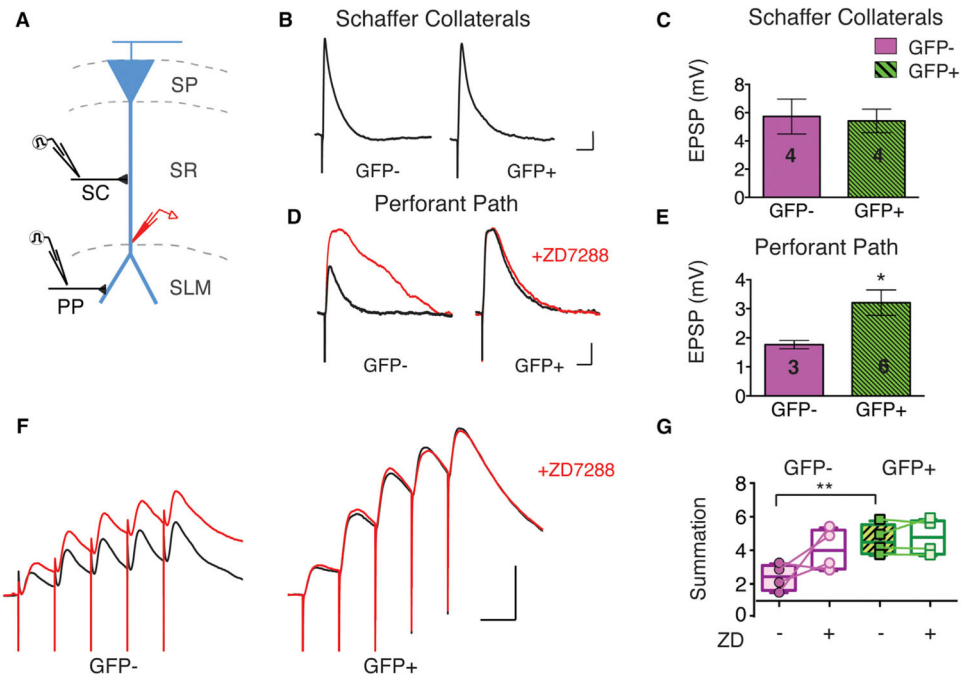

Figure 4. Dab1 Knockdown Reduces Integration of Synaptic Inputs Selectively in Distal Dendrites of CA1 PNs

(A) Experimental design: either the SC pathway or the PP was stimulated during whole cell current clamp voltage recordings from CA1 PN distal dendrites of Cre-GFP−or Cre-GFP+ neurons.

(B) Effect of Dab1 knockdown on EPSPs recorded in distal dendrites in response to stimulation of Schaffer collateral inputs, which target proximal dendrites. Example EPSPs shown for Cre-GFP−and Cre-GFP+ neurons. Scale bars, 1 mV, 50 ms.

(C) Dab1 knockdown had no significant effect on mean Schaffer collateral peak EPSP amplitude (unpaired t test, p = 0.842). Number of cells displayed on graph. (D) Effect of Dab1 knockdown on EPSPs recorded in distal dendrites evoked by stimulation of PP inputs, which target distal dendrites. Example EPSPs from Cre-GFP−and Cre-GFP+ CA1 neurons. Red traces show EPSPs obtained after application of 10 μM ZD7288 for each neuron. Scale bars, 1 mV, 50 ms.

(E) Dab1 knockdown significantly increased mean perforant path peak EPSP amplitude (p = 0.021).

(F) Effect of Dab1 knockdown on temporal summation of CA1 neuron EPSPs evoked by a burst of five perforant path stimuli delivered at 20 Hz. EPSPs recorded from Cre-GFP−and Cre-GFP+ neurons. Red traces show EPSPs recorded after application of 10 μM ZD7288. Scale bars, 5 mV, 50 ms.

(G) Mean summation of PP EPSPs recorded in Cre-GFP− and Cre-GFP+ neurons before and after ZD7288 application. Summation, measured as ratio of peak voltage during the fifth EPSP divided by peak voltage during the first EPSP, was significantly increased by Dab1 knockdown (**, p = 0.0097). In Cre-GFP+ neurons, ZD7288 had no effect (p = 0.401). Plot shows individual cells, min to max (whiskers), median (line), and 25th to 75th percentiles (box).

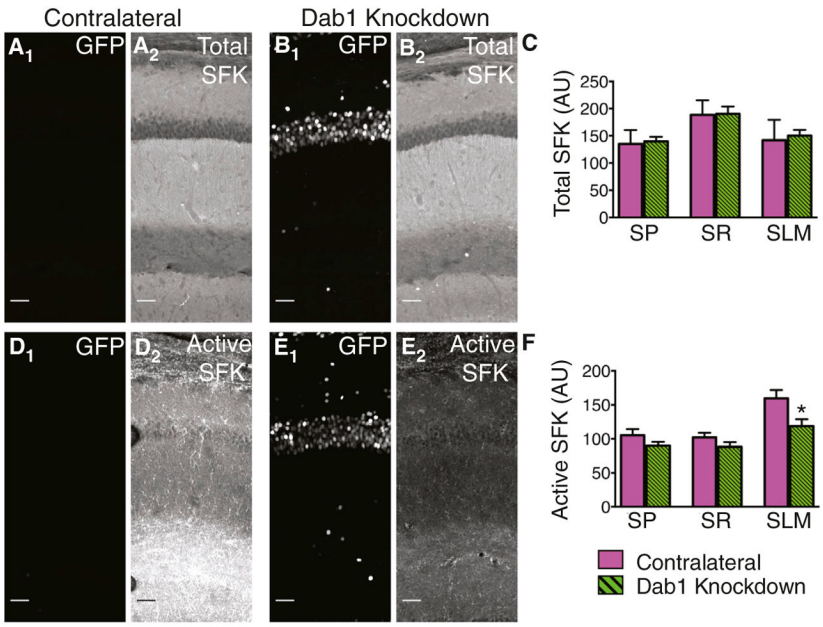

Figure 5. Regulation of SFK Activity by Dab1 In Vivo

(A) GFP signal (A_1) and total SFK staining (A_2) in a contralateral (control) hippocampus. To show the brain region in which the analysis was performed, maximum intensity z projection images were tiled. Scale bar, 50 μm for all images.

(B) GFP signal (B_1) and total SFK staining (B_2) in a Dab1 knockdown hippocampus.

(C) Mean intensity of total SFK staining was unaltered by Dab1 knockdown in all layers of CA1 (unpaired t tests: $p > 0.05$).

(D) GFP signal (D_1) and active SFK staining (D_2) in a contralateral hippocampus.

(E) GFP signal (E_1) and active SFK staining (E_2) in a Dab1 knockdown hippocampus.

(F) Mean intensity of active SFK staining was significantly reduced by Dab1 knockdown in SLM of CA1 ($p = 0.020$).

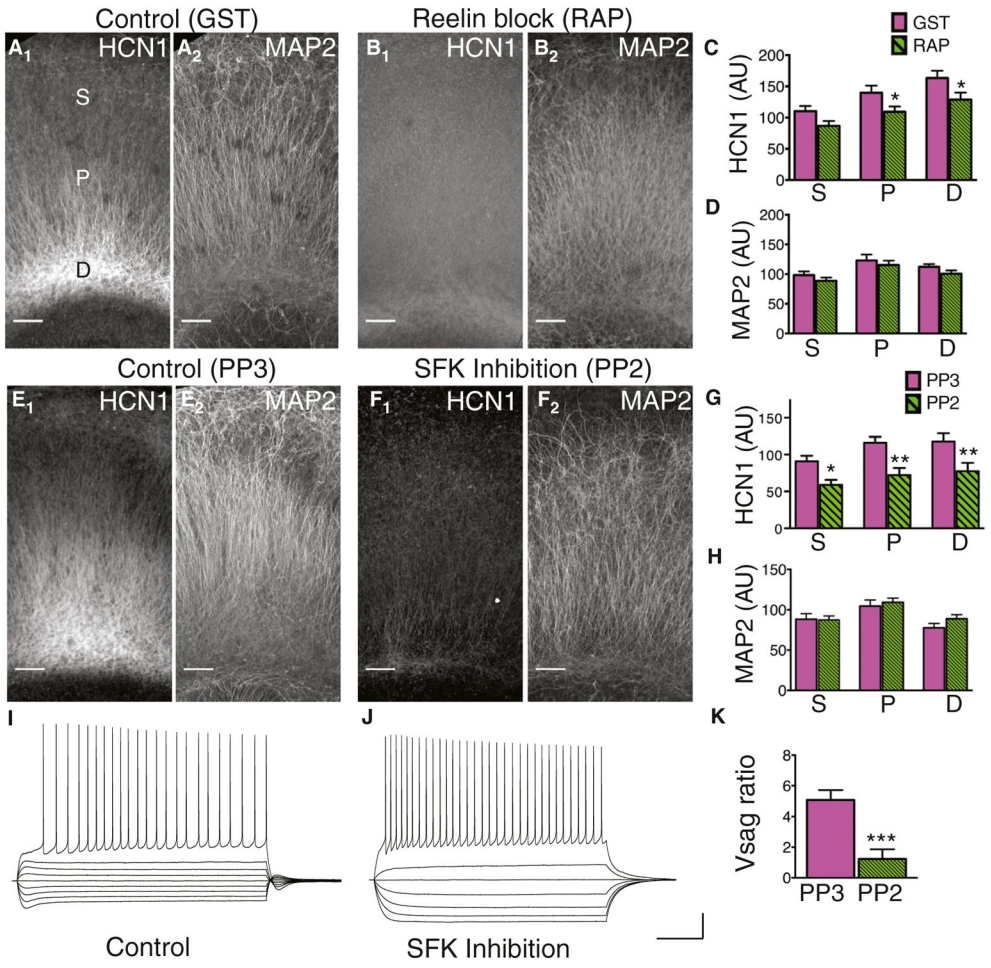

Figure 6. Effects of Reelin and SFK Inhibition on HCN1 Expression and Localization in Organotypic Cultures

(A) Image of the CA1 region from a control organotypic culture stained for HCN1 (A_1) and MAP2 (A_2). Somatic (S), proximal (P), and distal (D) regions of the apical dendrite are labeled in (A_1). To show the brain region in which the analysis was performed, maximum intensity z projection images were tiled. Scale bar, 100 μm for all images.

(B) Image of the CA1 region from an organotypic culture treated with RAP to block Reelin activity and stained for HCN1 (B_1) and MAP2 (B_2).

(C) Mean HCN1 intensity in the CA1 region of control and RAP-treated cultures. HCN1 was significantly reduced in proximal ($p = 0.040$) and distal regions ($p = 0.049$), but not in the somatic region ($p = 0.054$) of Dab1 knockdowns ($n = 12,19$).

(D) Mean MAP2 intensity was not significantly different in control and RAP-treated cultures.

(E) Image of the CA1 region from an organotypic culture treated with the inert analog PP3 and stained for HCN1 (E_1) and MAP2 (E_2).

(F) Image of the CA1 region from an organotypic culture treated with the SFK inhibitor PP2 and stained for HCN1 (F_1) and MAP2 (F_2).

(G) Mean HCN1 staining intensity in CA1 of PP3 (control) and PP2-treated cultures. HCN1 was significantly reduced in somatic ($p = 0.059$), proximal ($p = 0.003$), and distal ($p = 0.023$) regions in PP2 versus PP3-treated cultures ($n = 10,10$).
(H) Mean MAP2 intensity in PP2- and PP3-treated cultures.
(I) Whole cell current clamp voltage recording from a CA1 PN in a PP3-treated (control) culture in response to a series of hyperpolarizing and depolarizing current steps. Note prominent sag upon hyperpolarization. Scale bars, 20 mV, 200 ms (I and J).
(J) Whole cell current clamp voltage recording from a CA1 PN in a PP2-treated culture in response to identical current steps used in (I). Note lack of sag.
(K) Mean V_{sag} ratio was significantly reduced in PP2-treated versus PP3-treated control cultures ($p = 0.001$).

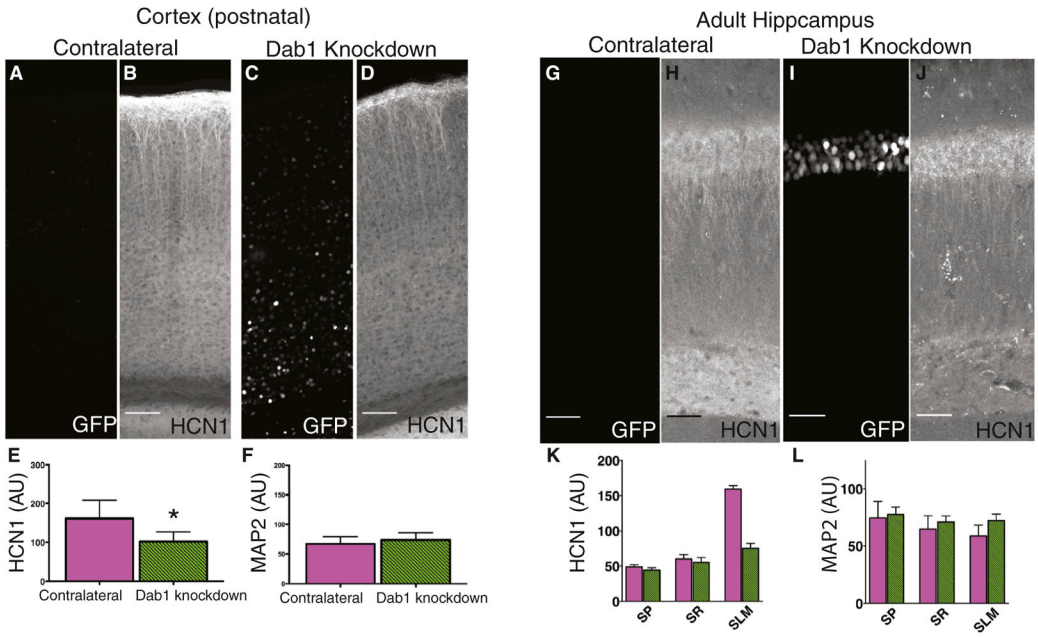

Figure 7. Knockdown of Dab1 Reduces HCN1 Expression in Distal Dendrites of Neocortical Neurons and in Hippocampi of Adult Injected Animals

(A) GFP signal in neocortex from hemisphere contralateral (Contra., control) to site of rAAV Cre-GFP injection. To show the brain region in which the analysis was performed, maximum intensity z projection images were tiled. Scale bar, 50 μm for all images.

(B) HCN1 staining in the contralateral neocortex. Strong staining in layer 1 reflects HCN1 enrichment in the distal apical tuft dendrites of layer 5 PNs.

(C) Cre-GFP signal in neocortex from hemisphere ipsilateral to site of injection. Cre-GFP+ neurons were observed in deep layers of the neocortex, including layer 5.

(D) Effect of Dab1 knockdown on HCN1 staining in neocortical slice.

(E) Mean HCN1 intensity in layer 1 was significantly reduced by Dab1 knockdown ($p = 0.025$) ($n = 6,6$).

(F) Dab1 knockdown caused no change in MAP2 staining intensity in layer 1 of neocortical slices obtained from contralateral or injected hemispheres. (G–J) GFP and HCN1 staining in an uninjected hippocampus (G and H) and a hippocampus in which rAAV Cre-GFP was injected during adulthood. (I and J). Scale bar, 50 μM in all images.

(K) Mean intensity of HCN1 was significantly reduced in SLM ($p = 0.0002$) in Dab1 knockdown hippocampi ($n = 4,4$). (L) Dab1 knockdown caused no change in MAP2 intensity in SP, SR, or SLM in hippocampi from adult injected animals.